Is it *really* a planet? Coupling Evidential Regression with Differentiable Rendering for JWST NIRCam PSF Characterization and Exoplanet Imaging

Edward Berman [1]   Rodrigo Ferrer-Chávez [2]   Aviad Levis [3]   Jason Wang [4]   Katherine Bouman [5]
Jacqueline McCleary [6]   William Freeman [7]   Brandon Feng [8]

Abstract

Modeling point-spread function (PSF) aberrations using differential forward models of optical systems fails to account for the inherent uncertainties in photometry, sky noise, and "unknown unknowns" in the forward model. While accurate PSF models are crucial for all sorts of astronomical analysis, the goal of this work is to create PSF models fordirect imaging of transiting exoplanets. In order to confirm an exoplanet planet discovery, we need a principled way to disambiguate planets from image artifacts such as hot pixels or dust. It is therefore of interest to quantify the uncertainty in our per-pixel predictions of the PSF model and whether we can leverage uncertainty quantification to produce a more reliable image of an exoplanet. In this work, we combine a differentiable forward model for the James Webb Space Telescope PSF with evidential regression so that we can model both the aleatoric and epistemic uncertainties of our PSF model. We coin our method EDDO-UQ, as an extension of the EDDO framework. We show the power of EDDO-UQ with clear direct detection of exoplanets using both simulated data and planet HIP 65426b.

1. Introduction

The James Webb Space Telescope Near Infrared Camera (JWST NIRCam) has unprecedented angular resolution, with pixel scales of $0.031''$/pixel and $0.063''$/pixel for the short and long wavelength channels, respectively. With JWST, we are now able to image not just galaxies and stars,

but even things as small scale as individual planets. To put this into perspective, the exoplanet HIP 65426b was recently imaged by Carter et al. (2023). The planet is 356 light years away and has a radius roughly the size of Jupiter. With a corresponding angular size of roughly 6.4×10^{-6} arcseconds and measuring using unresampled $F444W$ data, we can expect the planet to occupy $\frac{1}{1000}$ of a pixel on the detector. However, due to diffraction effects and small optical imperfections, as captured by the telescope point spread function (PSF), we are able to see the planetary light spread out over a few pixels!

The direct detection of HIP 65426b was accomplished computationally using pyKLIP (Wang et al., 2015). One of the core difficulties of direct exoplanet detection is that the light emanating from the transiting planet is of the same intensity of the speckle noise (Soummer et al., 2007) produced by the host star. pyKLIP attempts to model the star PSF in order to reveal the exoplanet behind the speckle noise.

Unfortunately, pyKLIP does not take into account the optical physics of JWST NIRCam, meaning it has the potential to make predictions that are non-physical. In response, subsequent works (e.g., Liaudat et al., 2023; Feng et al., 2025) have developed approaches to PSF characterization using differentiable optical models. These approaches optimize free parameters that are subject to the constraints imposed by the various instruments inside the telescope.

While these works have made great strides towards physically accurate PSF models, it can still be unclear when the PSF model is "good enough." That is to say, when subtracting off the effect of the PSF on a science image, it can be unclear whether the remaining artifact is truly an exoplanet or simply a combination of shot noise, read noise, and model misspecification (e.g., Golomb et al., 2021). The objective of this work is therefore to couple uncertainty quantification with differentiable rendering methods, which enables us to embed inductive biases from optical physics into our modeling while also modeling uncertainty. We take an approach rooted in evidential regression, which gives us a precise way of identifying the per-pixel uncertainties in our PSF model due to both model mispecification and detector noise. We coin our method Exoplanet Detection

*Equal contribution [1]Northeastern University [2]Northwestern University [3]University of Toronto [4]Northwestern University [5]California Institute of Technology [6]Northeastern University [7]Massachusetts Institute of Technology [8]Massachusetts Institute of Technology. Correspondence to: Edward Berman <berman.ed@northeastern.edu>.

with Differentiable Optics and Uncertainty Quantification (EDDO-UQ), as it extends the EDDO framework described in Feng et al. (2025). We show that EDDO-UQ is able to produce reliable uncertainty estimates of the PSF model on both real and simulated data, and furthermore that the uncertainty estimates themselves can be leveraged to make exoplanet detections easier. The remainder of this paper is organized as follows. In §2, we describe the methods of differentiable rendering and uncertainty quantification used in this work. We show the results of our method in §3. We offer conclusions in §4.

2. Method

Evidential Regression. Our primary method is the use of deep evidential regression to simultaneously model the per-pixel data (aleatoric) and model (epistemic) uncertainties[1] using the the formalism provided in Amini et al. (2020). Modeling of epistemic uncertainties is a core contribution of our method, since estimates of aleatoric (usually photometric) uncertainties often come with the JWST data products. However, the supplied aleatoric uncertainties can still be unreliable due to things like dust (Saydjari & Finkbeiner, 2022). It is therefore advantageous to have a model like EDDO-UQ that simultaneously estimates both.

We say that our data points $(y_1, \ldots, y_n) \sim \mathcal{N}(\mu, \sigma^2)$ and furthermore μ and σ^2 have priors

$$
\begin{aligned}
\mu &\sim \mathcal{N}(\gamma, \sigma^2 \nu^{-1}) \\
\sigma^2 &\sim \Gamma^{-1}(\alpha, \beta)
\end{aligned}
$$

where $\Gamma(\cdot)$ is the gamma function. Let $m = (\gamma, \nu, \alpha, \beta)$, and $\gamma \in \mathbb{R}, \nu > 0, \alpha > 1, \beta > 0$. One can then show that $p(y_i|m) = St(y_i; \gamma, \frac{\beta(1+\nu)}{\alpha\nu}, 2\alpha)$, where the St distribution is given by

$$
St(t; \mu, \sigma, \nu) = \frac{\Gamma\left(\frac{\nu+1}{2}\right)}{\sqrt{\pi\nu}\sigma\Gamma\left(\frac{\nu}{2}\right)} \left(1 + \frac{1}{\nu}\left(\frac{t-\mu}{\sigma}\right)^2\right)^{-(\nu+1)/2}.
$$

Characterizing the St distribution as a four-parameter family is useful because it allows us to define prediction, aleatoric uncertainty, and epistemic uncertainty in a rigorous way:

$$
\begin{aligned}
\mathbb{E}[\mu] &= \gamma \quad \text{(Prediction)}, \\
\mathbb{E}[\sigma^2] &= \frac{\beta}{\alpha - 1} \quad \text{(Aleatoric Uncertainty)}, \\
\text{Var}[\mu] &= \frac{\beta}{\nu(\alpha - 1)} \quad \text{(Epistemic Uncertainty)}.
\end{aligned}
$$

[1]Some fields refer to these as statistical and systematic uncertainties

In evidential regression, the goal is to learn the four-parameter family m that best describes the data $(y_1, \ldots, y_n)$ by minimizing the negative log likelihood $-\log p(y_i|m)$. This in turn gives us our prediction, aleatoric uncertainty, and epistemic uncertainty from a single training run.

Differentiable Forward Modeling. We use the differentiable forward model for the James Webb Space Telescope Near Infrared Camera (JWST NIRCam) described in Feng et al. (2025) for our prediction γ. Our differentiable renderer $\mathcal{G}$ takes as input the position of the guide star $p_{\text{star}} \in \mathbb{R}^2$ and a wavefront aberration map $\phi \in \mathbb{R}^{H_\phi \times W_\phi}$. $\mathcal{G}$ models four operations extracted from WebbPSF specifications (Perrin et al., 2014) in order to model NIRCam: We have the pupil entrance function $\mathcal{P}$, the focal plane mask $\mathcal{B}$, the Lyot Stop $\mathcal{C}$, and the NIRCam instrument $\mathcal{D}$. We will additionally use $\mathcal{F}$ to denote the Fourier transform. Our estimate of the science image is then

$$
\hat{\gamma} = |\mathcal{F}D \cdot \mathcal{C} \cdot \mathcal{F}\mathcal{B} \cdot \mathcal{F}\mathcal{P} \cdot (x^{(0)} \cdot e^{ip_{\text{star}}} \cdot e^{i\phi})|^2
$$

where $x^{(0)}$ is an input complex wavefront, typically a plane wave. For the purposes of this work, ϕ will be a grid of 1024×1024 learnable parameters.

Solving for the PSF. The negative log likelihood loss for $p(y_i|m)$ is known to be

$$
\begin{aligned}
\mathcal{L}_i^{\text{NLL}}(w) =& \frac{1}{2}\log\left(\frac{\pi}{\nu}\right) - \alpha\log(2\beta(1+\nu)) \\
&+ \left(\alpha + \frac{1}{2}\right)\log((y_i - \gamma)^2\nu + 2\beta(1+\nu)) \\
&+ \log\left(\frac{\Gamma(\alpha)}{\Gamma(\alpha + \frac{1}{2})}\right).
\end{aligned}
$$

We couple our negative log likelihood loss with a standard $L1$ regularization loss, which was shown to help training stability in Amini et al. (2020). This gives us

$$
\begin{aligned}
\mathcal{L}_i^{\text{R}}(w) &= |y_i - \mathbb{E}[\mu_i]| \cdot \Phi \\
&= |y_i - \gamma| \cdot (2\nu + \alpha) \\
\mathcal{L}_i(w) &= \mathcal{L}_i^{\text{NLL}}(w) + \mathcal{L}_i^{\text{R}}(w).
\end{aligned}
$$

We approximate $\hat{\gamma}$ with our differentiable renderer $\mathcal{G}$; however, our estimates for $\hat{\alpha}, \hat{\beta}, \hat{\nu}$ are almost entirely unconstrained. The estimates are modeled as a grid of learnable parameters the size of our predicted science image. We apply the softplus function to each and add 1 to $\hat{\alpha}$ to enforce the restrictions $\hat{\nu} > 0, \hat{\alpha} > 1, \hat{\beta} > 0$.
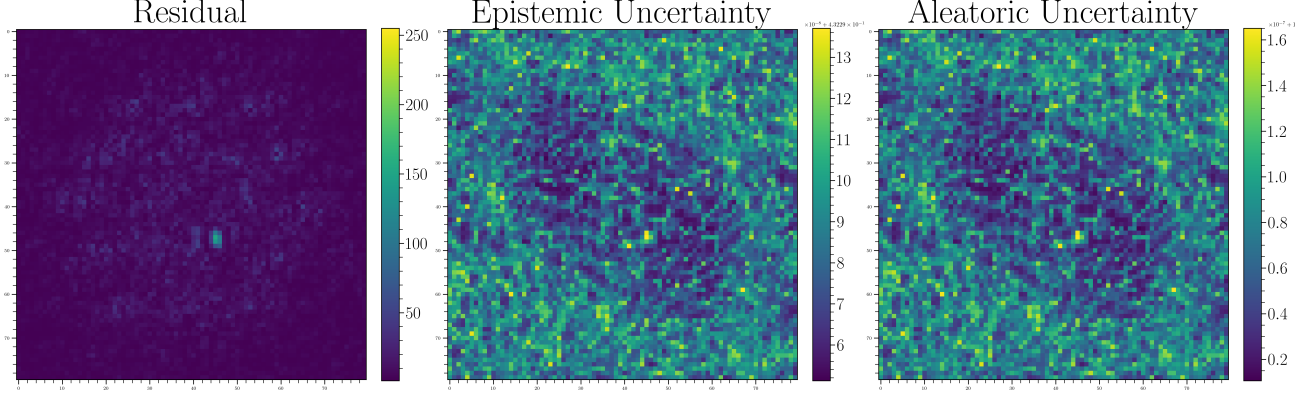
Figure 1. **Left:** The residual between image and PSF model. **Center:** The epistemic uncertainty. **Right:** The aleatoric uncertainty. The center color bar is in units of $\times 10^{-8} + 4.3229 \times 10^{-1}$ and the right color bar is in units of $\times 10^{-7} + 1$.

Once we have our trained model, we look for exoplanets in the residual of the image y and the PSF prediction γ. We can study the signal-to-noise with χ^2 images

$$\chi^2_{\text{al}} = \frac{(y - \hat{\gamma})^2}{\left(\frac{\hat{\beta}}{\hat{\alpha} - 1}\right)}$$

$$\chi^2_{\text{ep}} = \frac{(y - \hat{\gamma})^2}{\left(\frac{\hat{\beta}}{\hat{\nu}(\hat{\alpha} - 1)}\right)}.$$

To quantify the performance of EDDO-UQ, we set up a series of experiments featuring both simulated and real images of an exoplanet near a bright star. Our simulated data consists of 10 mock realizations of the planet-star system with controlled shot and read noise added to each realization. The initial star and wavefront abberations are rendered using an untrained EDDO and a hidden planet is manually added behind one of the speckles. Real images of the exoplanet HIP 65426b (Carter et al., 2023) are sourced directly from the Mikulski Archive for Space Telescopes we use data taken from MAST[2]. In our experiments, we train our model with a Cosine learning rate scheduler and AdamW optimizer. For simulated data we use 3000 epochs and for real data 6000 epochs.

3. Results

Simulated Data. This experiment confirmed that EDDO-UQ can identify an exoplanet in a simulated data setting. Interestingly, Figure 1 shows a spike in both uncertainty maps where the synthetic exoplanet is. This is unsurprising,

as the renderer $\mathcal{G}$ is meant to model speckle noise from the center guide star and not any other object. However, we are reassured by the fact that the uncertainty is still the same order of magnitude as the minimum, or in other words, that the uncertainty does not dominate the signal. Also of note is that the epistemic uncertainty less than the aleatoric uncertainty, which indicates that the inability to fit the data is bounded more by the read noise and shot noise than the expressivity of the model.

Exoplanet HIP 65426b. In this experiment, we establish that EDDO-UQ can directly detect exoplanets and that uncertainty estimation can help identify the planet. We study planet HIP 65426b (Carter et al., 2023) because it was recently imaged using the pyKLIP package (Wang et al., 2015), giving us a baseline to compare with. Notably, our planet location is consistent with what was found in Carter et al. (2023).

As seen in Figure 2, EDDO-UQ is able to reveal exoplanet HIP 65426b alongside its estimates for the epistemic and aleatoric uncertainties. Again, we find that the epistemic uncertainty is smaller than than the aleatoric uncertainty. When we weight the squared residuals by these uncertainties, as we do in Figure 3, we find that the hidden exoplanet becomes even more obvious. Put differently, our exoplanet signal is much higher than the noise, but very little of the surrounding pixels contain any signal compared to the noise.

The epistemic and aleatoric uncertainties are both highest around the center of the image. This is likely in accordance with the fact that the majority of the shot noise is in the center where the star shines most intensely, even if the coronagraph tries to mitigate that effect.
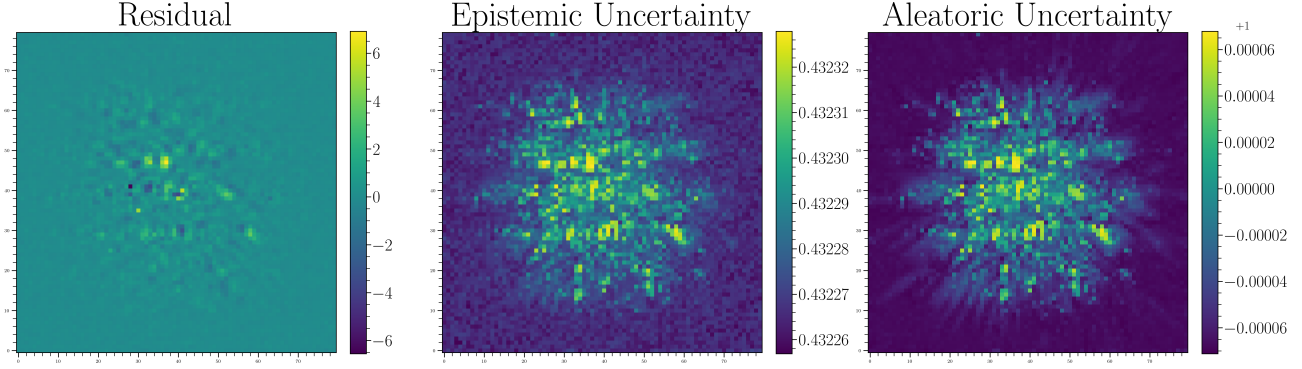
---

[2] https://webbtelescope.org/contents/media/images/01GBT1E93YV7YND5MFS1603FWJ

Figure 2. **Left:** The residual between image and PSF model. **Center:** The epistemic uncertainty. **Right:** The aleatoric uncertainty. As seen in the left panel, EDDO-UQ is able to successfully reveal the planet HIP65426b slightly up and to the left of the center of the image. Unlike pyKLIP, EDDO-UQ also produces estimates for the epistemic and aleatoric uncertainties.
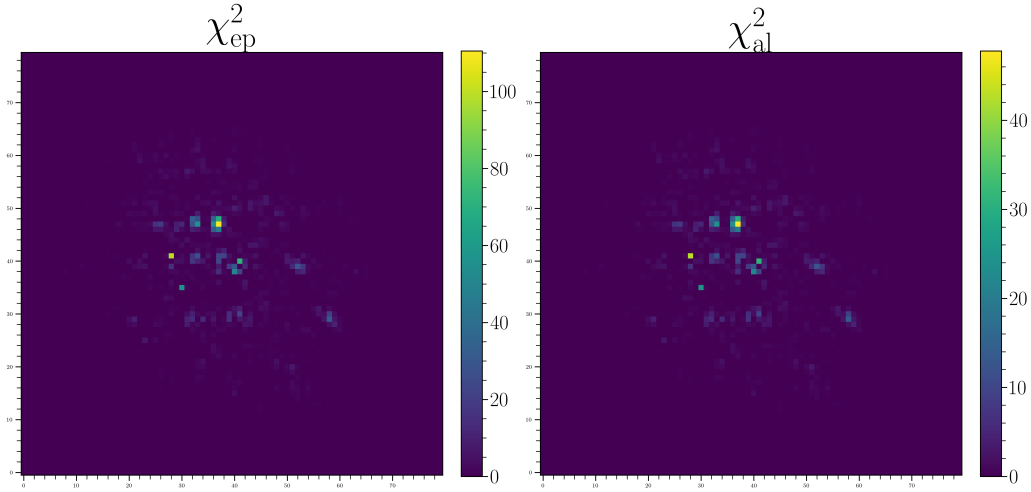

Figure 3. **Left:** The squared residuals weighted by the epistemic uncertainty. **Right:** The squared residuals weighted by the aleatoric uncertainty.

4. Discussion and Conclusions

In this work, we developed EDDO-UQ, a framework that couples uncertainty quantification with exoplanet detection with differentiable optics. We tested EDDO-UQ on both real and simulated data sets and demonstrated that by incorporating uncertainty estimation into our model, we can produce better and more contextualized science images. Our success can be partially explained by the results of (Seitzer et al., 2022). They show that including uncertainty parameters in the model causes the gradients of the loss function to preferentially impact the pixels where the uncertainty is low. Therefore, during the optimization loop, the parameters related to the pixels in the science image corresponding to

the core aberrations of the PSF are optimized more than the ones corresponding to background noise. This enables us to simultaneously learn a descriptive PSF model while also fitting uncertainty parameters.

More broadly, our work enables a more rigorous evaluation of candidate exoplanets as it allows users to simultaneously diagnose both modeling uncertainties and photometric uncertainties when fitting for the PSF. In turn, we can weight the final exoplanet image by the uncertainties and identify if our signal really dominates the noise. The epistemic uncertainties in particular provide an added measure of how reliable the PSF fit is, and the aleatoric uncertainties are useful in circumstances where the photometric measurements

are unreliable. Our work also enables likelihood analysis of observing a pixel under the learned St distribution, paving the way for future automated exoplanet detection.

References

Amini, A., Schwarting, W., Soleimany, A., and Rus, D. Deep evidential regression. *Advances in neural information processing systems*, 33:14927–14937, 2020.

Carter, A. L., Hinkley, S., Kammerer, J., Skemer, A., Biller, B. A., Leisenring, J. M., Millar-Blanchaer, M. A., Petrus, S., Stone, J. M., Ward-Duong, K., et al. The jwst early release science program for direct observations of exoplanetary systems i: High-contrast imaging of the exoplanet hip 65426 b from 2 to 16 μm. *The Astrophysical journal letters*, 951(1):L20, 2023.

Feng, B. Y., Ferrer-Chávez, R., Levis, A., Wang, J. J., Bouman, K. L., and Freeman, W. T. Exoplanet detection via differentiable rendering. *arXiv preprint arXiv:2501.01912*, 2025.

Golomb, J., Rocha, G., Meshkat, T., Bottom, M., Mawet, D., Mennesson, B., Vasisht, G., and Wang, J. Planetevidence: Planet or noise? *The Astronomical Journal*, 162(6):304, 2021.

Liaudat, T., Starck, J.-L., Kilbinger, M., and Frugier, P.-A. Rethinking data-driven point spread function modeling with a differentiable optical model. *Inverse Problems*, 39 (3):035008, 2023.

Perrin, M. D., Sivaramakrishnan, A., Lajoie, C.-P., Elliott, E., Pueyo, L., Ravindranath, S., and Albert, L. Updated point spread function simulations for jwst with webbpsf. In *Space telescopes and instrumentation 2014: optical, infrared, and millimeter wave*, volume 9143, pp. 1174–1184. SPIE, 2014.

Saydjari, A. K. and Finkbeiner, D. P. Photometry on structured backgrounds: Local pixel-wise infilling by regression. *The Astrophysical Journal*, 933(2):155, 2022.

Seitzer, M., Tavakoli, A., Antic, D., and Martius, G. On the pitfalls of heteroscedastic uncertainty estimation with probabilistic neural networks. *arXiv preprint arXiv:2203.09168*, 2022.

Soummer, R., Ferrari, A., Aime, C., and Jolissaint, L. Speckle noise and dynamic range in coronagraphic images. *The Astrophysical Journal*, 669(1):642, 2007.

Wang, J. J., Ruffio, J.-B., De Rosa, R. J., Aguilar, J., Wolff, S. G., and Pueyo, L. pyklip: Psf subtraction for exoplanets and disks. *Astrophysics Source Code Library*, pp. ascl–1506, 2015.